

MODELLING PHOSPHATES “DISTURBANCES” DEPTH USING ANALYTICAL SIGNAL RESPONSES OF GEOELECTRICAL RESISTIVITY DATA (SIDI CHENNANE, MOROCCO): PRELIMINARY RESULTS

Saad BAKKALI¹, Mahacine AMRANI²

¹Earth Sciences Department Geosciences, Faculty of Sciences and Techniques, Tangier, MOROCCO

²Engineering Process Department, Faculty of Sciences and Techniques, Tangier, MOROCCO

Abstract

Exploitation of the phosphate layers in Sidi Chennane deposit (Morocco) collides frequently with problems bound to the existence, in the phosphate series, of sterile bodies qualified as *derangements*. Our study shows that these bodies, masked by the Quaternary cover can be mapped using the geoelectrical prospecting survey. A Schlumberger resistivity survey over an area of 50 hectares was carried out. A new field procedure based on analytic signal response of resistivity data was tested to deal with the presence of phosphate deposit disturbances. Models of the geology were successfully obtained from surface modelling of 2D peaks of resistivity data. Image processing optimization was based on surface optimization tools. Downward analytical continuation of the surface modelling along 30 meters depth was used for modelling Sidi Chennane phosphates “disturbances” distribution. Analytical procedures were found to be consistently useful. Optimization of phosphate reserves were improved and better constrained.

Key words: resistivity, phosphate, analytic signal, downward, Morocco.

1. GEOPHYSICAL AND GEOLOGICAL SETTINGS

Resistivity is an excellent parameter and marker for distinguishing between different types and degree of alteration of rocks. Resistivity surveys have long been successfully used by geophysicists and engineering geologists and the procedures are well established. The study area is the Ouled Abdoun phosphate basin which contains the Sidi Chennane deposit (figure 1). The Sidi Chennane deposit is sedimentary and contains several distinct phosphate-bearing layers. These layers are found in contact with alternating layers of calcareous and argillaceous hardpan. However, the new deposit contains many inclusions or lenses of extremely tough hardpan locally known as “*derangements*” or “*disturbances*” (figure 2), found throughout the phosphate-bearing sequence [1].

Figure.1. (A) Location of the studied area in the sedimentary basin of Ouled Abdoun. (B) Section showing the disruption of the exploitation caused by disturbances. (C) Stratigraphical log of the phosphatic series of Sidi Chennane: (1) Hercynian massif; (2) phosphatic areas; (3) marls; (4) phosphatic; marls; (5) phosphatic layer; (6) limestones; (7) phosphatic limestone; (8) discontinuous silex bed; (9) silex nodule; (10) *dérangement* formed exclusively of silicified limestone; (11) *dérangement* constituted of a blend of limestone blocks, marls and clays; (12) *dérangement* limit; (13) roads.

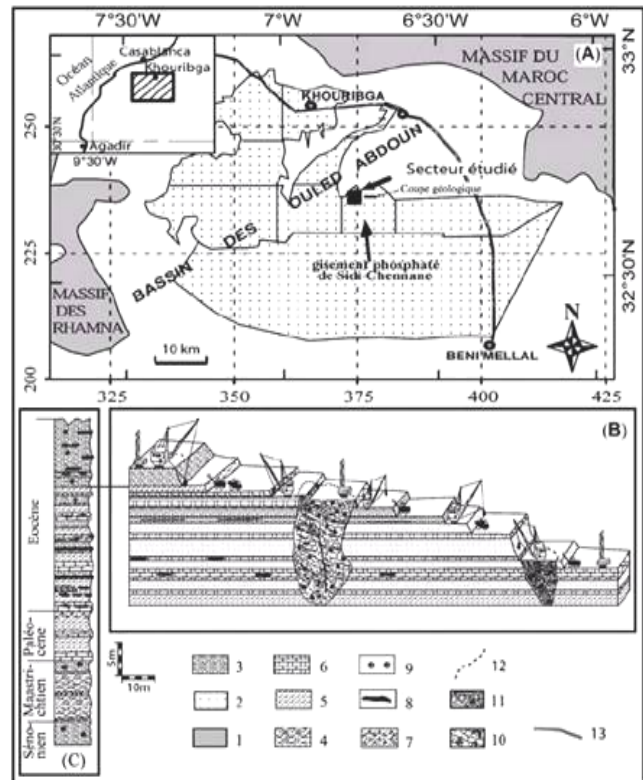




Figure.2. Examples of “disturbances” in the phosphatic series

The hardpan pockets are normally detected only at the time of drilling. Direct exploration methods such as well logging or surface geology are not particularly effective. They interfere with field operations and introduce a severe bias in the estimates of phosphate reserves (figure 3).

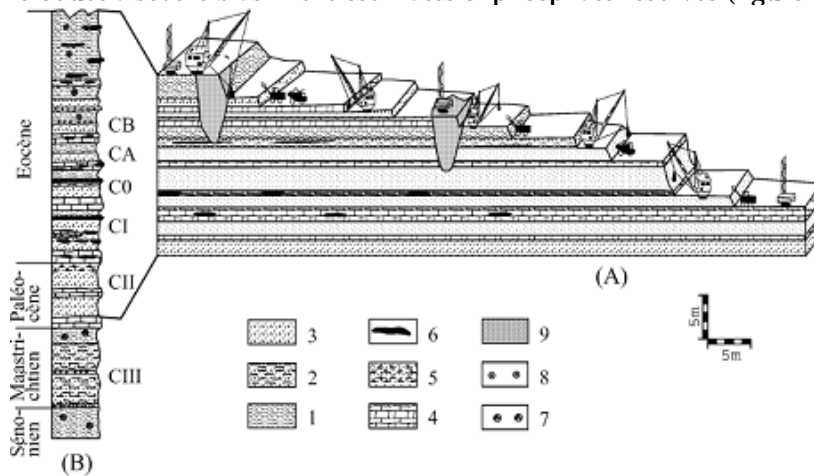


Figure.3. A. Section showing the disruption of the exploitation caused by sterile bodies. B. Stratigraphical log of the phosphatic series of Sidi Chennane: 1, marls; 2, phosphatic marls; 3, phosphatic layer; 4, limestones; 5, phosphatic limestone; 6, discontinuous silex bed; 7, calcite concentration; 8, silex nodule; CIII, CII, C1, C0, CA, CB: exploited phosphatic layers; 9, sterile body

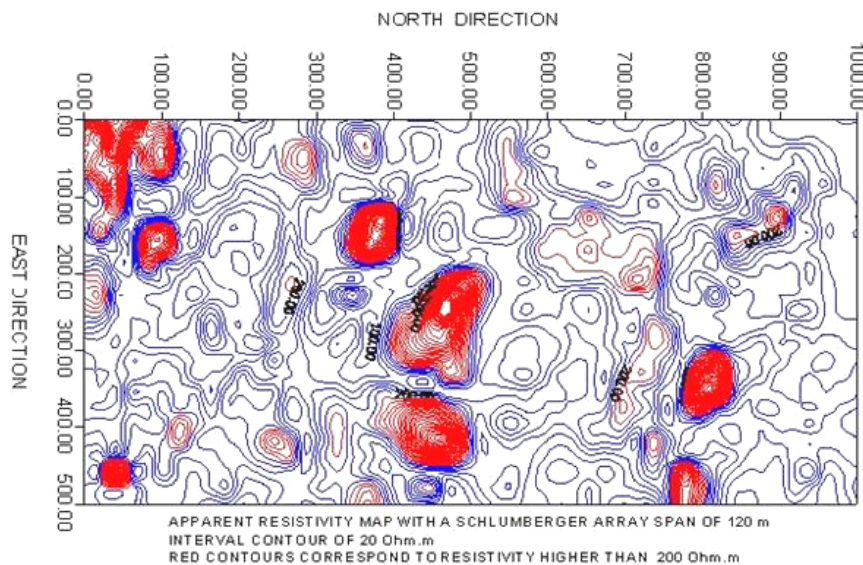


Figure.4. A map of resistivity anomalies for AB=120 m (distances in meters).

The study area was selected for its representatively and the resistivity profiles were designed to contain both disturbed and enriched areas. The sections were also calibrated by using vertical electrical soundings. High values of apparent resistivity were encountered due to the presence of near-vertical faulting between areas of contrasting resistivity, and fault zones which may contain more or less highly conducting fault gouge. The gouge may contain gravel pockets or alluvial material in a clay matrix. Such anomalous sections are also classified as *disturbances*. Apparent resistivity values in these profiles locally exceeded 200 Ω .m. [2][3]. The apparent resistivity map (figure 4) obtained from a further survey was considered in fact a map of discrete potentials on the free surface, and any major singularity in the apparent resistivity due to the presence of a perturbation will be due to the crossing from a “normal” into a “perturbed” area or vice versa. In other words, the apparent resistivity map may be considered a map of scalar potential differences assumed to be harmonic everywhere except over the perturbed areas. Interpretation of resistivity anomalies is the process of extracting information on the position and composition of a target mineral body in the ground. In the present case the targets were essentially the inclusions called perturbations. The amplitude of an anomaly may be assumed to be proportional to the volume of a target body and to the resistivity contrast with the mother lode. If the body has the same resistivity as the mother lode no anomaly will be detected. The resistivity anomalies would be representative of the local density contrast between the “disturbances” and the mother lode. Level “disturbance” of the anomalous zones is proportional to resistivity intensity (figure 4) [4][5].

2. THE FIELD PROCEDURES

Resistivity is an excellent parameter and marker for distinguishing between different types and degree of alteration of rocks. Resistivity surveys have long been successfully used by geophysicists and engineering geologists and the procedures are well established. The study area was selected for its representatively and the resistivity profiles were designed to contain both disturbed and enriched areas. The sections were also calibrated by using vertical electrical soundings. High values of apparent resistivity were encountered due to the presence of near-vertical faulting between areas of contrasting resistivity, and fault zones which may contain more or less highly conducting fault gouge. The gouge may contain gravel pockets or alluvial material in a clay matrix [6]. Such anomalous sections are also classified as *disruption or disturbances*. Apparent resistivity values in these profiles locally exceeded 200 Ω .m. In order to locate and define the anomalous areas or *disturbances corresponding to resistivity anomalies*, an electric current of intensity I was passed between electrodes A and B , and the voltage drop ΔV was measured between the potential electrodes M and N . The apparent resistivity is found from $\rho_{app}=K(\Delta V/I)$, where K is the geometric constant of the instrument which depends only on the distance between electrodes [7]. Thus the ratio between I and ΔV yields the resistivity of the terrain. Our Schlumberger set required the electrodes to be aligned and equidistant from the central point O so that $MN \ll AB$. The longer the section, the deeper is the sensitivity of the survey. The lateral in homogeneities of the ground can be investigated by means of the apparent resistivity obtained from the survey. As the surface extension of the layers is displayed we may infer the presence or absence of any disturbances as well as any geological setting variations. Our resistivity measurements were performed by means of a Syscal2 resistivity meter by BRGM Instruments using a rectangular array of 20 m x 5 m. In order to reach a mean depth of exploration of 40 m we carried out 51 traverses at a spacing of 20 m (figure 5). There were 101 stations at 5 m distance for every traverse, which makes 5151 stations all together in the survey [7].

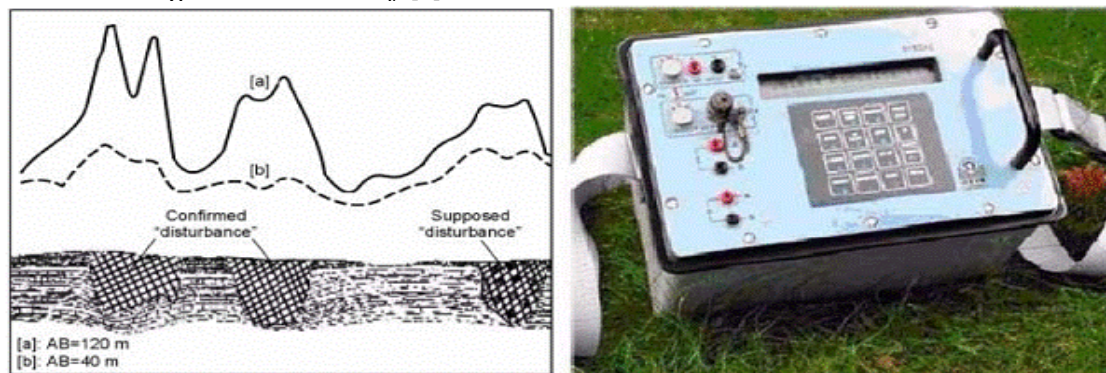


Figure.5. A synthetic apparent resistivity traverses over three disturbances (left side) and the Syscal resistivity meter used in the study (right side).

3. THE ANALYTIC SIGNAL METHOD

Apparent resistivity measurements are obtained from a harmonic potential V which fulfills Laplace's equation $\Delta V=0$ in the surrounding space external to the body. The potential gradient falls off as $1/r^2$ [8]. As a first approximation, the scalar potential in the neighborhood of the perturbations and within the sources complies with the equation $\Delta V=-2\rho I \delta(r)$, where $\delta(\cdot)$ is the Dirac delta, ρ is the resistivity in the anomalous region and I is the current at a point electrode in an elastic half space, i.e. the topographic surface of the study area [9]. The apparent resistivity map which one obtains from such a survey is actually a map of discrete potentials on the free surface, and any major singularity in the apparent resistivity due to the presence of a perturbation will be due to the crossing from a "normal" into a "perturbed" area or vice versa. In other words, the apparent resistivity map may be considered a map of scalar potential differences assumed to be harmonic everywhere except over the perturbed areas. Interpretation of resistivity anomalies is the process of extracting information on the position and composition of a target mineral body in the ground. In the present case the targets were essentially the inclusions called *perturbations*. The amplitude of an anomaly may be assumed to be proportional to the volume of a target body and to the resistivity contrast with the mother lode. If the body has the same resistivity as the mother lode no anomaly will be detected. The resistivity anomalies would be representative of the local density contrast between the disturbances and the mother lode. Level "disturbance" of the anomalous zones is proportional to resistivity intensity [10] (figure 6).

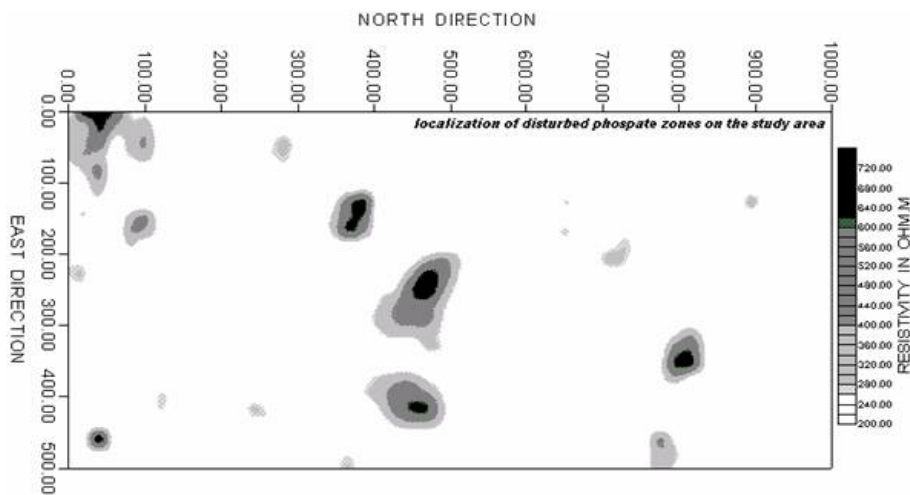


Figure.6. A map of disturbed phosphate zones corresponding to figure 5

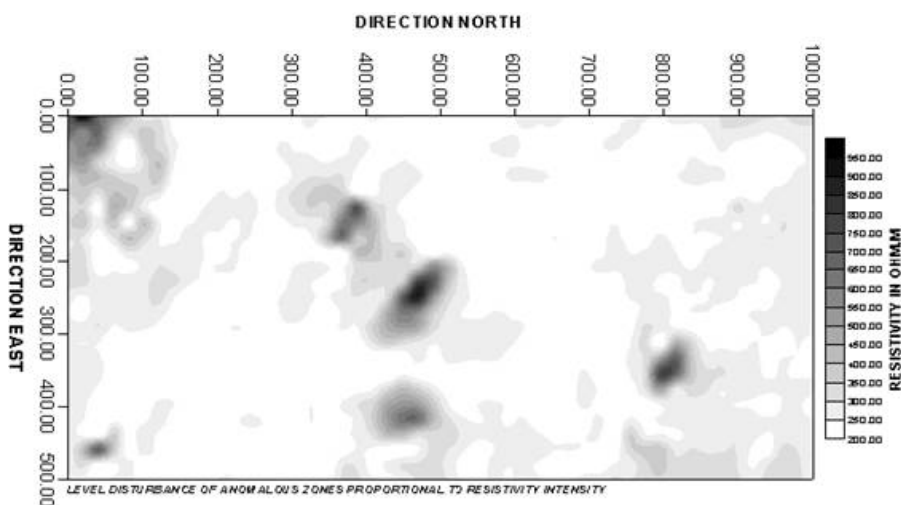


Figure.7. Analytical signal response of figure 6

The horizontal and the vertical derivatives of the resistivity anomalies produced by a potential source form a Hilbert transform pair and define an analytic signal [11]. The analytical processing method also called the total gradient method is used for defining the edges of density anomalies in terms of spatial derivatives in orthogonal directions. An important property of the 3D analytic signal is

that its amplitudes define the envelope of its underlying signal [12]. It follows that the magnitude of the gradient of resistivity data is seemed to be equal to the envelope of both the horizontal and vertical derivatives over all possible directions. For processing resistivity data, the amplitude of the analytic signal in 3D is remarkable in that it allows one to obtain a representative signal of the resistivity anomalies over all possible directions on the study area (figure 7).

Mapped maxima in the calculated analytic signal map locate the anomalous source body edges witch correspond basically to the anomalous zones of phosphate deposit “disturbances”. Analytic signal maxima have the useful property that they occur directly over singular contacts regardless of structural dip which may be present. The amplitude of the 3D analytic signal, or the total gradient, is indeed the envelope over all possible directions [13]. Let $A(\rho)$ be the analytic signal of the apparent resistivity both in the East and North directions. We suppose $A(\rho)$ a function of x, y and ϑ defined as :

$$A(\rho(x, y)) = a(x, y) \cos \vartheta + b(x, y) \sin \vartheta \quad (1)$$

where $a(x, y)$ and $b(x, y)$ are the directional derivatives respectively in the easting and the northing:

$a(x, y) = \frac{\partial \rho(x, y)}{\partial x}$ and $b(x, y) = \frac{\partial \rho(x, y)}{\partial y}$. So equation (1) can be expressed by the following terms:

$$A(\rho(x, y)) = \frac{\partial \rho(x, y)}{\partial x} \cos \vartheta + \frac{\partial \rho(x, y)}{\partial y} \sin \vartheta \quad (2)$$

x and y are the cartesian parameters of the study area, and ϑ one of all possible directions. The envelope of the analytic signal of the apparent resistivity function over all values of ϑ can be obtained by taking the derivative of $A(\rho)$ with respect to ϑ , setting it to zero, solving for ϑ as a function of $\frac{\partial \rho(x, y)}{\partial x}$ and $\frac{\partial \rho(x, y)}{\partial y}$, and substituting this expression into the definition of the apparent resistivity function [14] :

$$\sin \vartheta = \frac{\pm \frac{\partial \rho(x, y)}{\partial y}}{\sqrt{\left(\frac{\partial \rho(x, y)}{\partial x}\right)^2 + \left(\frac{\partial \rho(x, y)}{\partial y}\right)^2}} \quad (3)$$

$$\cos \vartheta = \frac{\pm \frac{\partial \rho(x, y)}{\partial x}}{\sqrt{\left(\frac{\partial \rho(x, y)}{\partial x}\right)^2 + \left(\frac{\partial \rho(x, y)}{\partial y}\right)^2}} \quad (4)$$

Substituting the expressions for $\cos \vartheta$ and $\sin \vartheta$ into equation (1) we obtained the surface envelope peaks denoted

$$\varepsilon |A(\rho(x, y))| = \sqrt{\left(\frac{\partial \rho(x, y)}{\partial x}\right)^2 + \left(\frac{\partial \rho(x, y)}{\partial y}\right)^2} \quad (5)$$

An equivalent of equation (5) is given by the following equation:

$$\varepsilon |A(\rho)| = \sqrt{|\rho|^2 + \left(\frac{\partial \rho}{\partial \vartheta}\right)^2} \quad (6)$$

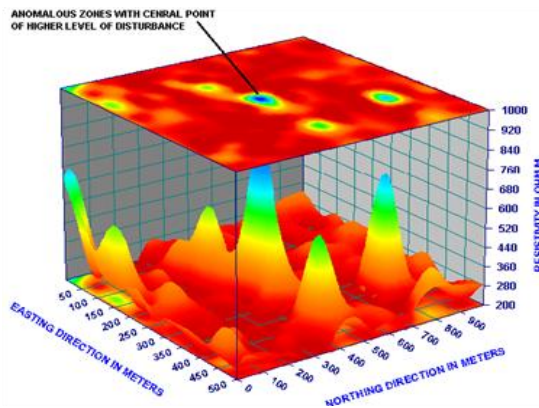
Partial derivatives are computed numerically. The horizontal gradients are usually estimated by finite difference methods from values measured at gridded points on the apparent resistivity anomaly map using the following equations:

$$\frac{\partial \rho(x, y)}{\partial x} = \frac{\rho_{i+1, j} - \rho_{i-1, j}}{2\delta x} \quad \text{and} \quad \frac{\partial \rho(x, y)}{\partial y} = \frac{\rho_{i, j+1} - \rho_{i, j-1}}{2\delta y}$$

where x is the eastern coordinate and y the northern coordinate. $\rho_{i, j}$ is the pseudo-apparent resistivity defined at grid point (i, j) [15]. Grid intervals in the x -direction and y -direction are δx and δy respectively. In others terms surface envelope peaks are given by the following equation:

$$\left(\varepsilon|A(\rho)\right)_{i,j} = \sqrt{\left(\frac{\rho_{i+1,j} - \rho_{i-1,j}}{2\delta x}\right)^2 + \left(\frac{\rho_{i,j+1} - \rho_{i,j-1}}{2\delta y}\right)^2} \quad (7)$$

We interpolate numerically the different peaks by a surface-fit graph which defines the surface envelope of the resistivity data corresponding to the anomalous zones of the phosphate deposit disturbances [16]. The surface-fit graph is the central point in the TableCurve 3D software used [17]. This graph will display the x, y and $\varepsilon|A(\rho(x, y))$ data along the surface for a fitted and given equation. Since optimizations are such an important part of surface science, the surface min and



surface max check boxes allow for the display x, y and $\varepsilon|A(\rho(x, y))$ coordinates of the minimum and maximum of the surface [18]. These are found by a two dimensional optimization algorithm (figure 8).

Figure.8. 3D resistivity peaks surface modeling corresponding to phosphate deposit “disturbances” zones.

Figure 8 represents in this case an indicator of the level of variation of the contrast of density between the disturbances and the normal phosphate-bearing rock. The surface modeling of resistivity anomalies is obtained by the TableCurve 3D routine from our apparent resistivity survey. This procedure enables us

to define the sources, after a sequence of filtering operations by analytic signal. These procedures are basically spatial filters which enhance some features of the anomaly map at the expense of other features, thus enabling us to connect the surface anomalies to the sources at depth proportionally to resistivity peaks on the study’s area [19]. The contrasting of density between the disturbances and the normal phosphate-bearing rock attest that the disturbances are contrasted on the surface. The overall effect is that of scanning the anomalous bodies. Downward analytic continuation will also amplify the effect of the deep structures, and enables us to separate the effect of adjacent sources [20]. To some extent it enables us to obtain an outline of the anomalous structures and, in any case, to find the depth to the roof of the body. Of course there is a possibility to confuse several structures with a single structure. The data are imaged symmetrically in the space domain in order to minimize edge effects on the transformed map. Otherwise some spurious high frequency effects may appear around the edges. The downward continuation operator may be expressed in the frequency domain by a factor $e^{-2\pi v z}$, where z is the targeted depth. The frequency v may be defined as $v = \sqrt{u^2 + v^2}$, where u and v are the frequencies in the East and North directions [21][22].

Once the resistivity map was filtered in the frequency domain the downward-prolonged map at a depth of 30 m was restored back to the space domain by inverse Fourier transform. Downward continuation was carried out in steps of 5 meters which enabled us to sample the entire sequence of the phosphate formation.

4. RESULTS

The normalized surface resistivity maps as obtained by the above procedure in the study area provided a direct image for an interpretation of the resistivity survey (figure 9). We were able to identify the anomalies which turned out to be strongly correlated with the disturbances. We found that the disturbances as detected from surface measurements were distributed apparently at random.

The map of resistivity anomalies was enhanced with the analytical signal procedure. The anomalous areas were neatly outlined. The disturbances were outlined in depth down to 30 m. The high resistivity over anomalous areas are interpreted as reflecting the fact that the pockets of disturbed material tend to become more consolidated at depth with a less extension as modeled by the surface interpolation. We find that the downward analytic continuation approach procedure helps to better constrain the surface location of anomalous areas. We also found that the extension in depth of the anomalous zones of phosphate deposit disturbances is limited and seem not to have an increased consistency as outlined by the downward analytical continuation of the surface modeling. As resistivity survey with a Schlumberger device of 120 m had target 40 meters depth, it appears according to surface modeling that the anomalous zones of phosphate deposit disturbances were clearly described in the pilot study area.

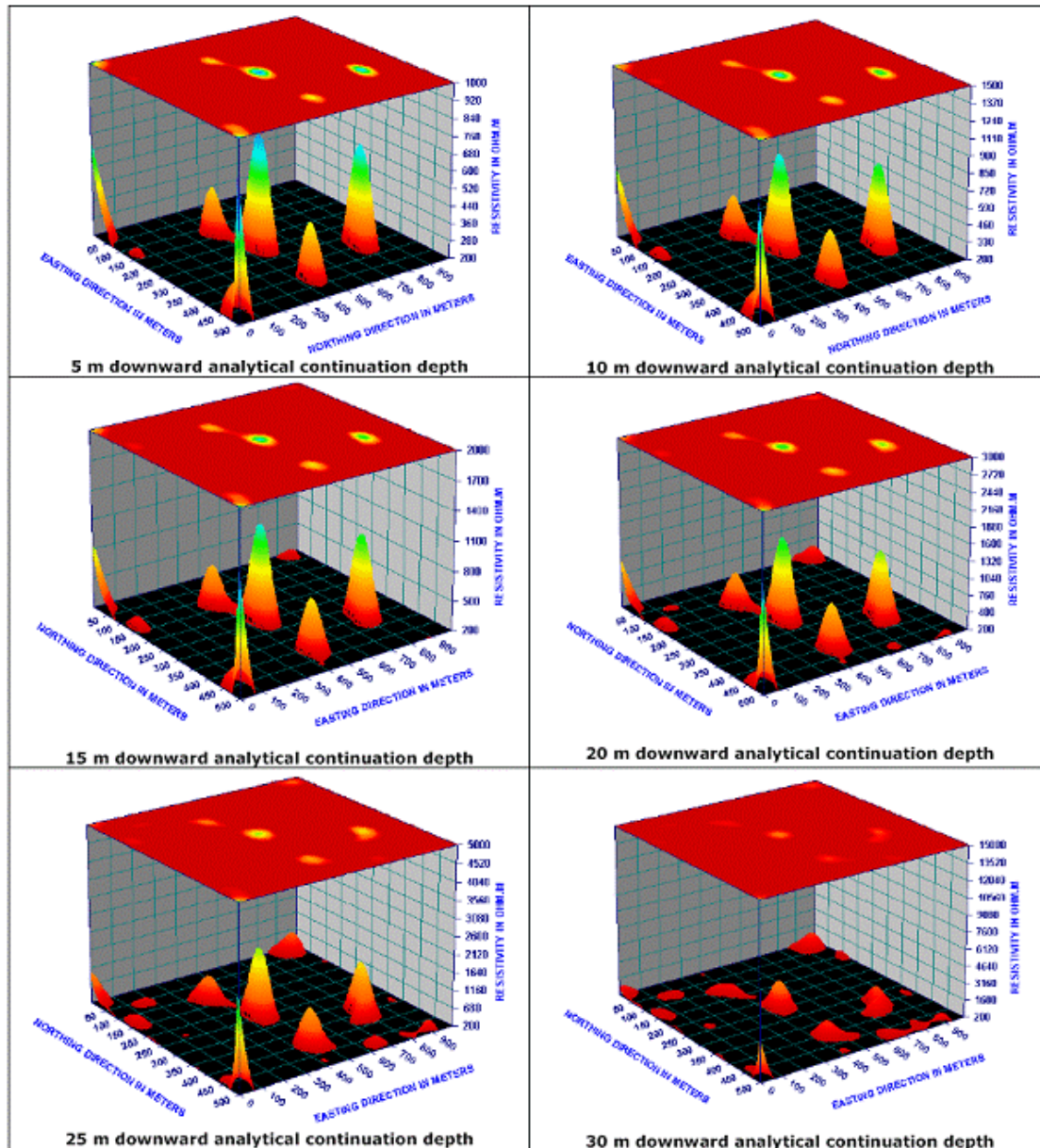


Figure.9. Downward analytic continuation resistivity peaks surface modeling corresponding to Figure.8.

5. CONCLUSIONS

We have described an analytical procedure to identify the anomalies of a specific problem in the phosphate mining industry. The results proved satisfying. Data processing procedures as surface “disturbances” modeling using optimization of 2D peaks analytic signal of resistivity data were found to be consistently useful and the corresponding maps may be used as auxiliary tools for decision making under field conditions. The downward analytical continuation of the surface disturbances modeling may be used by the operating personnel as a kind of radar to plan the sequence of field operations. The maps of surface “disturbances” modeling were particular useful to the surveyors for improving and constraining their 3D estimates of phosphate reserves in the deposit.

REFERENCES

- [1] Kchikach, A., Jaffal, M., Aifa, T. and Bahi, L. Cartographie de corps stériles sous couverture quaternaire par méthode de résistivités électriques dans le gisement phosphaté de Sidi Chennane (Maroc). *Comptes Rendus, Geosciences*, 2002, 334, 379-386.
- [2] Bakkali, S. Analysis of phosphate deposit “disturbances” using the horizontal-gradient responses of resistivity data (Oulad Abdoun, Morocco), *Earth Sci. Res. J.*, 2005, Vol.9, N°2, 123-131.

- [3] Bakkali, S. and L. Bahi. Cartographie des « dérangements » de séries phosphatées par mesures de résistivités électriques, *Journal des Sciences Pour l'Ingénieur, J.S.P.I.*, 2006, 6, 1-10.
- [4] Bakkali, S. Application du filtrage spatial à l'analyse des contours des zones anormales de « dérangements » des séries phosphatées de Sidi Chennane (Maroc), *Revue Afrique Science*, 2006, Vol.2, N°2, 116-130.
- [5] Bakkali, S. A resistivity survey of phosphate deposits containing hardpan pockets in Oulad Abdoun, Morocco, *Geofisica Internacional*, 2006, 45 (1), 73-82.
- [6] Kchikach, A., Andrieux, P., Jaffal, M., Amrhar, M., Mchichi, M., Boya, B., Amaghazaz, M., Veyrieras, T., Iqizou, K. Les sondages électromagnétiques temporels comme outil de reconnaissance du gisement phosphaté de Sidi Chennane (Maroc): apport à la résolution d'un problème d'exploitation. *Comptes Rendus, Geosciences*, 2006, 338, 289-296.
- [7] Telford, W. M., Sheriff, R.E. *Applied Geophysics*, Cambridge University Press, 1991, 790 p.
- [8] Blakely, R.J. *Potential Theory in Gravity and Magnetic Applications*, Cambridge University Press, 1995, 441 p.
- [9] Cooper, G., Cowan, D. The application of fractional calculus to potential field data *Exploration Geophysics*, 34, 2003, 51-56.
- [10] Bakkali, S., Amrani, M. About the use of spatial interpolation methods to denoising Moroccan resistivity data phosphate "Disturbances" map. *Acta Montanistica Slovaca*, 2008, 13 (2), 216-222.
- [11] Nabighian, M.N. The analytic signal of two dimensional bodies with polygonal cross section : its properties and use for automated anomaly interpretation, *Geophysics*, 37, 1972, 507.
- [12] Kanasewich, E.R. *Time sequence analysis in Geophysics*, The University of Alberta Press, 1981, 480 p.
- [13] Xiong, L. Understanding 3D analytic signal amplitude. *Geophysics*, 71 (2), 2006, P. L13-L16.
- [14] Zauderer, E. *Partial Differential Equations of Applied Mathematics*, 3rd Ed, Wiley-Interscience, New Jersey, 2006, 930 p.
- [15] Bakkali, S. Analysis of phosphate deposit "disturbances" using the horizontal-gradient responses of resistivity data (Oulad Abdoun, Morocco). *Earth. Sci. Res. J.* , 2005, 9 (2), 123-131.
- [16] Salem, A., Ravat, Dhananjay., Gamey, T.J., Ushijima, K. Analytic signal approach and its applicability in environmental magnetic investigations. *Journal of Applied Geophysics*, 2002, 49, 231-244.
- [17] Systat, 2002, About TableCurve 3Dl software version 4.0, Manuel d'utilisation, Copyright Systat Software Inc, 1993-2002.
- [18] Ardestani, E. V., Motavalli Anbaran, H. Constraints of analytic signal to determine the depth of gravity anomalies. *Journal of the Earth & Space Physics*, 33 (2), 2007, P. 135.
- [19] Pawlowski, R.S. Preferential continuation for potential-field anomaly enhancement. *Geophysics*, 60 (2), 1995, 390-398.
- [20] Trompat, H., Boschetti, F., Hornby, P. Improved downward continuation of potential field data. *Exploration Geophysics*, 2003, 34(4), 249-256.
- [21] Syberg, F.R.J. A Fourier method for the regional-residual problem of potential fields. *Geophysical Prospecting*, 20, 1972, 47-75.
- [22] Phillips, J.D. Potential-field continuation: past practice vs. modern methods. 66th Meeting, SEG, 1996, Denver, Expanded Abstracts, 1411-1414.

